Supplementary material: Daily prefrontal closed-loop repetitive transcranial magnetic stimulation (rTMS) produces progressive EEG quasi-alpha phase entrainment in depressed adults

Josef Faller*[1], Jayce Doose*[2], Xiaoxiao Sun*[1,3], James R. Mclntosh[1,4], Golbarg T. Saber[5,6], Yida Lin[7], Joshua B. Teves[5], Aidan Blankenship[5], Sarah Huffman[8], Robin Goldman[9], Mark S. George[8,10], Truman R. Brown[2,5], and Paul Sajda[1,11,12,13]

[1]Department of Biomedical Engineering, Columbia University, New York, NY 10027, USA
[2]Center for Biomedical Imaging, Medical University of South Carolina, Charleston, SC 29425, USA
[3]Human Research and Engineering Directorate, US DEVCOM Army Research Laboratory, Aberdeen Proving Ground, MD 20115, USA
[4]Department of Orthopaedic Surgery, Columbia University Irving Medical Center, New York, NY 10032, USA
[5]Department of Radiology and Radiological Science, Medical University of South Carolina, Charleston, SC 29425, USA
[6]Department of Neurology, University of Chicago, Chicago, IL 60637, USA
[7]Department of Computer Science, Columbia University, New York, NY 10027, USA
[8]Department of Psychiatry and Behavioral Sciences, Medical University of South Carolina, Charleston, SC 29425, USA
[9]Center for Healthy Minds, University of Wisconsin-Madison, Madison, WI 53705, USA
[10]Ralph H. Johnson VA Medical Center, Charleston, SC 29401, USA
[11]Department of Radiology, Columbia University Irving Medical Center, New York, NY 10032, USA
[12]Department of Electrical Engineering, Columbia University, New York, NY 10027, USA
[13]Data Science Institute, Columbia University, New York, NY 10027, USA
*contributed equally

February 21, 2022

S.1 Determining preferred alpha phase using a combined fMRI-EEG-TMS (fET) system

Each patient underwent a simultaneous fET scan at the beginning of the study to determine a subject-specific preferred alpha phase which evoked strongest activity in dorsal anterior cingulate cortex (dACC). They also underwent a second fET scan at the end of their treatment (after 30 sessions) to determine the preferred phase after the treatment was complete. Simultaneous EEG was recorded using a custom-built MR-compatible EEG system [1–3]. A 3T Siemens Prisma MRI

scanner (Siemens, Munich, Germany) was used to collect functional echo-planar image (EPI) data. A comprehensive description of the hardware along with preprocessing and analysis of EEG data can be found in [2]. A Rapid2 system (Magstim, Whitland, UK) was used for TMS pulse delivery and the timing of delivery was controlled via a custom E-Prime 2 (Psychology Software Tools, PA, USA) program synchronized with the scanner trigger. Stimulator intensity was set at 120 % of the subject's motor threshold. Each TMS pulse was fired at the beginning of a 200 ms gap at the end of each TR (i.e., repetition time in fMRI pulse sequence). In a subsequent analysis, the corresponding phase of frontal alpha was estimated in the EEG at the time of each TMS pulse. The preferred phase was then selected as the phase that was associated with the strongest response in the dACC as measured by the BOLD (blood oxygen level dependent) signal.

We hypothesized that the level of activation of the anterior cingulate cortex (ACC) varies following a transcranial magnetic stimulation (TMS) pulse applied to the DLPFC, with a dependence on the precise timing of the applied TMS pulses relative to the phase of the individual subject's EEG alpha rhythm (in practice, we expanded the EEG frequency range to 6 to 13 Hz for the alpha phase-locking in the EEG-rTMS system, and therefore refer to this rhythm as "quasi-alpha" EEG in the manuscript). To maximize the effect of the weeks of EEG-synchronized Repetitive TMS (rTMS) in this clinical trial, we thus determined a "preferred phase" (i.e., the target phase in the EEG quasi-alpha cycle relative to which we triggered the first TMS pulse of a rTMS pulse train if this individual is assigned to the SYNC group) once initially when subjects were enrolled using a combined fET instrument that we developed [4]. Specifically, we use EEG to estimate the instantaneous subject specific alpha phase in frontal regions covering the DLPFC prior to TMS pulse delivery, and measure activity in the ACC BOLD signal to assess target engagement.

We model the phase as ϕ, a phase shift between the alpha rhythm and BOLD response as the symbol alpha α^c, and the BOLD response as y:

$$y = b_0^c + A \cdot \cos(\alpha^c + \phi) \tag{1}$$

$$\Leftrightarrow y = b_0^c + A\cos\alpha^c \cos\phi - A\sin\alpha^c \sin\phi \tag{2}$$

$$\Leftrightarrow y = b_0^c + b_1^c \cos\phi + b_2^c \sin\phi \tag{3}$$

where $b_1^c = A\cos\alpha^c$, and $b_2^c = -A\sin\alpha^c$. Since $\sin^2(\alpha) + \cos^2(\alpha) = 1$, we can derive that $(\frac{b_1^c}{A})^2 + (\frac{-b_2^c}{A})^2 = 1 \Rightarrow A = \sqrt{(b_1^c)^2 + (b_2^c)^2}$. In addition, we can derive, based on tangent function, that $\tan(\alpha^c) = \frac{\sin\alpha^c}{\cos\alpha^c} = \frac{-b_2^c/A}{b_1^c/A} = \frac{-b_1^c}{b_2^c}$.
Rewriting this formula in matrix form, we obtain the model:

$$Y = XB^c + \varepsilon \tag{4}$$

$$\Leftrightarrow \begin{bmatrix} y_0 \\ y_1 \\ \dots \\ y_n \end{bmatrix} = \begin{bmatrix} x_0^0 & x_0^1 & x_0^2 \\ x_1^0 & x_1^1 & x_1^2 \\ \dots & \dots & \dots \\ x_n^0 & x_n^1 & x_n^2 \end{bmatrix} \times \begin{bmatrix} b_0^c \\ b_1^c \\ b_2^c \end{bmatrix} + \varepsilon \tag{5}$$

where $x_i^0 = 1$, $x_i^1 = \cos\phi$ and $x_i^2 = \sin\phi$.

Using the equations above, we explain the BOLD response with a sinusoidal model of phase. The maximum of the sinusoid from this model for the first fET scan, gives us our pre-treatment preferred phase (ϕ_{pre}) for each subject, and it was used as the target phase (ϕ_{targ}) of TMS pulse triggering in the EEG-rTMS treatment sessions for subjects in the SYNC group. This method is repeated using a Bayesian approach to generate estimates of how much we can trust the estimates of coefficients mapping phase to the BOLD response. A report of the preferred phase calculation

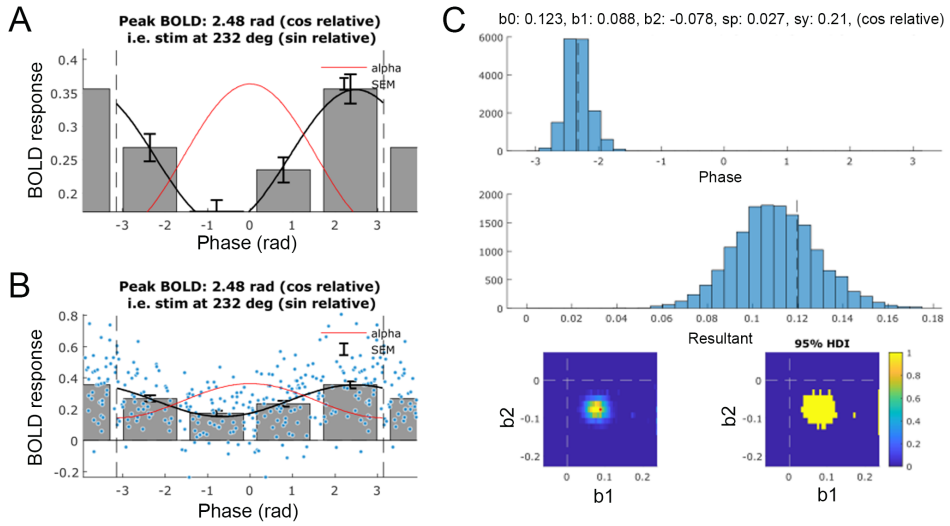

Figure S.1: Example report of the preferred phase estimation. Panel A shows the result of modelling BOLD response as a sinusoid relative to the alpha oscillation. The histogram shows binned response with standard error of the mean (SEM). The black line represents the model fit while the red line shows the corresponding alpha oscillation which is defined entirely by the x-axis. In this case, peak BOLD is reached at 2.48 rad relative to a cosine which means 4.06 rad relative to a sine function. Panel B is the same as A, but with raw data (blue dots) overlaid. Panel C includes a Markov Chain Monte Carlo (MCMC) result which provides an idea of the confidence we have in our parameter estimates. Parameters recovered by MCMC are $b_0 = 0.123$, $b_1 = 0.088$, and $b_2 = -0.078$ with $sp = 0.27$ and $sy = 0.21$, so the MCMC peak is at 2.30 rad relative to a cosine which is 222 degrees relative to a sine function. $p(b_1 = b_2 = 0)$ is outside 95% highest density interval (HDI) and approximate HDI for $p(b_1 = b_2 = 0)$ is 100%.

for each subject was generated (see Figure S.1). The preferred phase that we derived was used over the subsequent weeks of EEG-rTMS treatment if and only if this subject was assigned to SYNC group. For instance, Figure S.1 includes one subject's model result of assumed model described in Equation (5) above, where $b_0 = 0.254$, $b_1 = 0.062$, $b_2 = -0.080$ relative to a cosine, so we are targeting a peak at 2.48 rad relative to a cosine function (i.e., 4.06 rad relative to a sine function). Because all our preferred phases of each subject are determined relative to a sine function, this subject should be stimulated at 232 degrees ($\phi = 4.06$ rad $= \frac{4.06}{\pi} \times 180^\circ \approx 232^\circ$) relative to a sine wave if they belong to the SYNC group (SYNC: $\phi_{targ} = \phi_{pre}$). For subjects that were assigned to the UNSYNC treatment group, a random value for ϕ_{targ} was drawn and targeted for every first TMS pulse in each rTMS pulse-train (UNSYNC: $\phi_{targ} \sim U(0, 2\pi)$). At the end of all treatment sessions, a second fET scan was done to measure the post-treatment preferred phase (ϕ_{post}) for each subject with the same estimation method described above.

S.2 System used for closed-loop EEG guided rTMS

To administer rTMS locked to the phase of the target oscillation in the EEG, we improved upon an earlier custom-built system [4, 7] with similar capability. The software read densely sampled (10 kHz) EEG from the amplifier in chunks of 20 samples. After applying a causal finite impulse response (FIR)-based antialiasing filter [8] with a cut-off frequency at 50 Hz, the EEG data was downsampled to 500 Hz by retaining only every 20^{th} sample. Next, the left lateralized prefrontal alpha oscillation was recovered by first spatially averaging the signal for the EEG channels F3, F7 and FP1 and by applying a causal FIR based band-pass filter with corner frequencies at

$IAF \pm 2\,\text{Hz}$. The software then fit a model based on a single sinusoid (i.e., on the features $\sin(2\pi \times f \times t)$ and $\cos(2\pi \times f \times t)$) to the filtered signal in the time window [-300, ∼-100] ms using ordinary least squares regression. The algorithm allowed for flexibility in terms of the exact frequency by first fitting the model for multiple frequencies. Candidate frequencies were f_c where $\{f_c \in \mathbb{R} | f_c = IAF - 3 + \xi + 0.5 \times k \; and \; f_c < IAF + 3\}$ for $k = 0...12$ and where ξ was drawn randomly from a uniform distribution over the range 0 to 0.5 ($\xi \sim U(0, 0.5)$). The frequency in f_c that was associated with the lowest RMSE fit was used to predict the signal for a test window [-100, 0] ms. The time point for the next peak in the IAF rhythm was predicted and scheduled for future triggering of an rTMS pulse train only if the RMSE between prediction and signal in the test window were under a specific subject specific threshold (see S.4 in for details of threshold determination). The logic continued to pre-process data, but no new model fitting attempts were started until the scheduled time-point was reached. Once the scheduled time point was reached, an rTMS pulse train was triggered via parallel port output from the control computer to a microcontroller-based safety monitoring circuit, which ensured stimulation could not go above 14 Hz maximum or 3000 pulses total for a given treatment session. Each of the 40 pulses in a pulse train was individually triggered with a delay between pulses of $1/IAF$. Triggering was always followed by a refractory period of $2 \times 40 \times (1/IAF)$, so that the OFF time following stimulation was at minimum 2 times the length of the ON time for stimulation (see Figure 1 in main manuscript). During this refractory period, new EEG data was preprocessed but sine fitting and hence triggering remained disabled.

S.3 Determining TMS intensity for closed-loop EEG-rTMS

The resting motor threshold (MT) was measured at the beginning of the first treatment session. TMS pulses for all treatment sessions was delivered using a Magstim Horizon system (Magstim, Whitland, UK). MT was acquired using single pulse TMS which provides a noninvasive index of cortical excitability. The parameter estimation by sequential testing (PEST) approach [9] was chosen for threshold estimation. A motor response to TMS was defined as any finger movement in the right hand. For PEST determination, a pulse was delivered at a certain intensity and then the experimenter had to report whether or not they observed a motor response. This process was repeated in subsequent trials until the PEST algorithm converged to a precise resting MT estimate. During treatment, TMS intensity was gradually configured from measured subject-specific MT up to 120 % of this MT (1^{st} session 100% MT, 2^{nd} session 110% MT, and 3^{rd}+ session 120% MT). The scalp location over the left DLPFC that was targeted with rTMS was determined by taking measurements with the EEG cap on. Nasion to inion, tragus to tragus and head circumference were measured which are then input into the Beam F3 software. This then provides two coordinates, distance along circumference from midline (X) and distance from vertex (Y), which were used to identify the location of F3, which is then marked on a personalized swim cap for reference for future treatment sessions [10].

S.4 Determining individual alpha frequency (IAF) and triggering threshold

Many characteristics of the EEG, including the frequency of the alpha oscillation, can show high variability across individuals. Given the non-stationary nature of the EEG data, these characteristics can change between (or even within) a day for an individual. This presents challenges for real-time phase tracking in patients undergoing treatment.

In our study, every treatment session started with a "resting state" recording of five minutes of EEG, for which patients were instructed to keep their eyes open and visually fixate on a point marked by a grey cross (18cm wide, 18cm tall, 2 cm line thickness), 110 inches in front of them. This recording was used to determine the IAF, picked from a range between 6 and 13 Hz, as determined by baseline EEG power. This recording was further used to optimize individual thresholds for triggering TMS, represented by a model fit parameter called Root Mean Square Error (RMSE). This optimization was done to ensure that the system did not take longer than approximately 5 seconds to identify an appropriate EEG target, which ensures that delivering 3000 TMS pulses in one treatment session would take no more than approximately 30 minutes. An identical five-minute resting state recording was collected at the end of each treatment session.

Typically, rTMS treatment sessions last around 30 min per day. This is significant, since a standard course of rTMS treatment lasts for six to seven weeks, with daily treatment. Patients' EEG alpha peaks and alpha power generally stayed fairly consistent across treatment sessions. However, to account for daily variability, the individual alpha frequency (IAF) and triggering threshold were recalculated at the start of every daily treatment session. For this process, 5 minutes of eyes open resting state EEG were recorded every day prior to treatment. Especially, the daily adjustment of the triggering threshold also helped to optimize the trade-offs between overall session duration and TMS pulse firing accuracy.

rTMS was always delivered at the daily IAF frequency (the time of inter pulse interval $t_{ipi} = 1/IAF$), measured as the strongest point in the alpha band which is defined between 6 and 13 Hz. Here, we describe how the IAF was determined from the first five minutes of resting state EEG that we recorded daily: First, we separated data into 4 second epochs and ignored the first and the last epochs. After that, we performed outlier removal. In order to identify outliers, epoch offset was subtracted by individual and mean squared signal in each trial was calculated. Trials, in which the signal at at least one time point exceeded 2.5 $\times$ mean absolute deviation (MAD) above the median were defined as outliers. Then, we subtracted global mean, calculated power spectral density (PSD) of each epoch by using a hamming window and averaged across the PSDs for these epochs. Additionally, we applied the "fooof" function [11, 12] on the mean of the PSD, for the fit bounds between 3.5 to 24 Hz, and calculated the $1/f$ noise. Lastly, we subtracted the $1/f$ noise from the mean of the PSD and identified the maximum in the range from 6 to 13 Hz. The summary of IAF by subject is available in Table S.1. In addition, the comparison of IAF between SYNC and UNSYNC group by session is shown in Figure S.2. When pooling the resulting IAFs for all sessions across subjects for the SYNC group and separately for the UNSYNC group, an independent samples t-test for IAF between the two groups found no significant difference ($p = 0.1077$).

For triggering rTMS pulse trains, the real-time rTMS-EEG system uses an algorithm to identify when a prediction of the future phase of the signal is robust enough so as to achieve accurate phase targeting. Through pilot experiments, we found that it was critical to adapt triggering thresholds of this algorithm to the subject's EEG, so that rTMS was triggered often enough (i.e., 75 pulse trains) within one 30 min treatment session. To enable this adaptation, we created a program to optimize these trade-offs between targeting accuracy and treatment session time. In general, this program would identify a threshold value (i.e., Root Mean Square Error; RMSE) based on a series of simulations, with the objective that the real-time targeting algorithm would take approximately 5 seconds to identify an appropriate target. Specifically, these simulations entailed running the EEG-rTMS real-time algorithm (see Figure 1 in main manuscript) at different triggering thresholds (i.e., RMSE). So like during real-time processing (see section S.2), the algorithm fit a sine based model to a time window at [-300, ∼-100] ms and tested the resulting model on a time window at [-100, 0] ms. Provided the RMSE between prediction and actual signal in the test window was smaller than the triggering threshold, simulated triggering was scheduled for up to 123 ms into

Subject	Condition	mean(μ)	SD(σ)	$IAF_{1^{st}}$	quasi-α $power_{1^{st}}$	$ITPC_{1^{st}}^{max[1]}$
P01	unsync	10.34	0.56	10.7	9.8	0.28
P02	unsync	8.35	0.48	8.5	3.2	0.10
P03	unsync	11.10	0.85	11.2	2.6	0.08
P04	unsync	8.39	0.57	8.8	0.15	0.45
P05	unsync	11.10	0.89	10.3	1.5	0.48
P06	unsync	9.54	0.36	9.5	8	0.21
P07	unsync	7.30	1.20	6.3	1.6	0.23
P08	unsync	6.95	0.43	6.8	5.6	0.28
P09	sync	6.88	0.53	8.5	1.5	0.21
P10	sync	7.02	0.48	6.8	2.2	0.34
P11	sync	7.94	0.78	9	13	0.13
P12	sync	10.67	0.84	10.3	14	0.23
P13	sync	8.48	0.67	9	6.1	0.20
P14	sync	8.23	1.88	6.1	0.75	0.47
P15	sync	10.82	0.82	12	0.25	0.23

Table S.1: Summary of IAFs by subject (Unit: Hz). Mean(μ) and standard deviation(σ) of IAFs for each subject are presented. There were four sessions (session #8, #19 #23 and #26) from subject P10 where the IAF could not be determined at the beginning of that treatment. In these four sessions, the IAF from the previous session was used for treatment. The specific values of the IAF, the corresponding quasi-α power and the first post-TMS ITPC peak of session #01 are also listed. These values are used for a correlation test to investigate possible differences between the two treatment groups with respect to these variables. (Note: all powers shown above are baseline (mean) subtracted and 1/f noise removed.)

Condition	Correlation	Pearson's ρ	p-value
sync	IAF : quasi-alpha power	0.26	0.57
sync	quasi-alpha power : $ITPC^{max[1]}$	-0.55	0.20
sync	IAF : $ITPC^{max[1]}$	-0.66	0.10
unsync	IAF : quasi-alpha power	0.23	0.59
unsync	quasi-alpha power : $ITPC^{max[1]}$	-0.26	0.54
unsync	IAF : $ITPC^{max[1]}$	-0.01	0.98

Table S.2: Results of correlation tests among IAF, quasi-alpha power that associated with IAF and $ITPC^{max[1]}$. The results of p-value show that there is no significant linear correlation between IAF and its associated quasi-alpha power. Moreover, it shows that there is no significant linear correlation between quasi-alpha power and $ITPC^{max[1]}$ that we used to represent post-TMS phase entrainment.

the future. Other EEG preprocessing details matched those during real-time processing: EEG was re-referenced based on right mastoid (electrode TP10) and the 3 frontal electrodes (FP1, F3 and F7). A 200 Hz low pass filter was applied causally, the group delay was accounted for to match the real-time system, and the EEG was downsampled from 10 KHz to 500 Hz. The IAF was calculated based on the method introduced above. Causal detrending was applied by calculating the mean of the signal within a time window [-100, 0] ms and by subtracting that mean from the value at time point 0. The bandpass filter of 6 to 13 Hz was selected to match the subject's IAF and the associated group delay was taken into account in the triggering logic. As a major difference to the real-time logic, the simulations used a much lower refractory period so as to use the 5 minutes of calibration data as efficiently as possible.

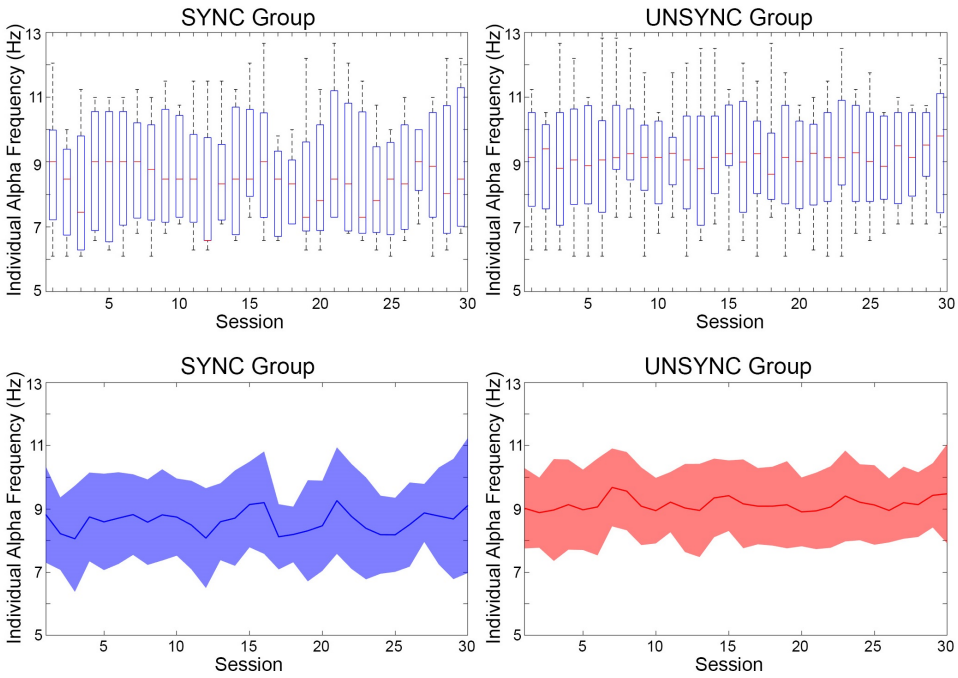

Figure S.2: Distribution and changes of IAFs over sessions by group. The top row shows boxplots of IAFs by session for each group. The figures in the bottom row show the mean IAF across participants and over all sessions. The shaded areas (SYNC: blue, UNSYNC: red) indicate standard errors across subjects within each group.

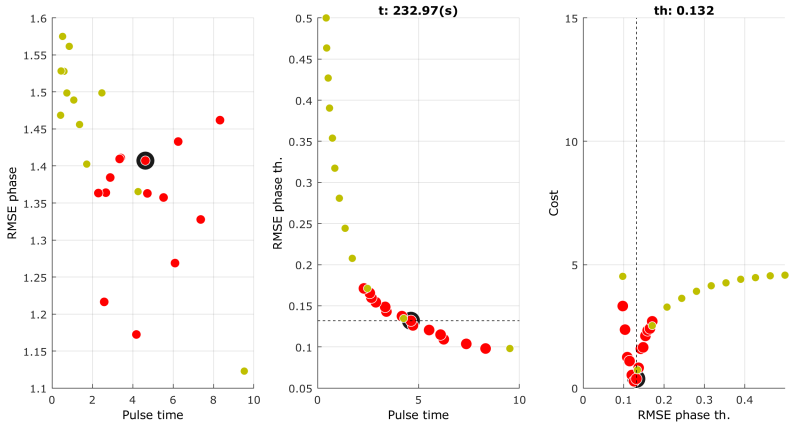

Figure S.3: RMSE phase threshold calculation. The lowest cost point is selected, which is shown as black circle in the panel on the right. It corresponds to the black circle in the center panel where the associated RMSE phase threshold and pulse time are shown. The plot on the left, finally, shows where the point falls in terms of RMSE phase.

By considering Table 3 in main manuscript together with Table S.1, we see that even though there is no significant correlation between IAF and ITPC^{max}[1] based on the statistical result of the GLMM, we see that the SYNC subjects (#P09 and #P10) who have the most significant phase entrainment increase are also the subjects who have a relatively low average IAF across sessions (6.88 Hz and 7.02 Hz). To further investigate the possible effects of the IAF and its associated alpha

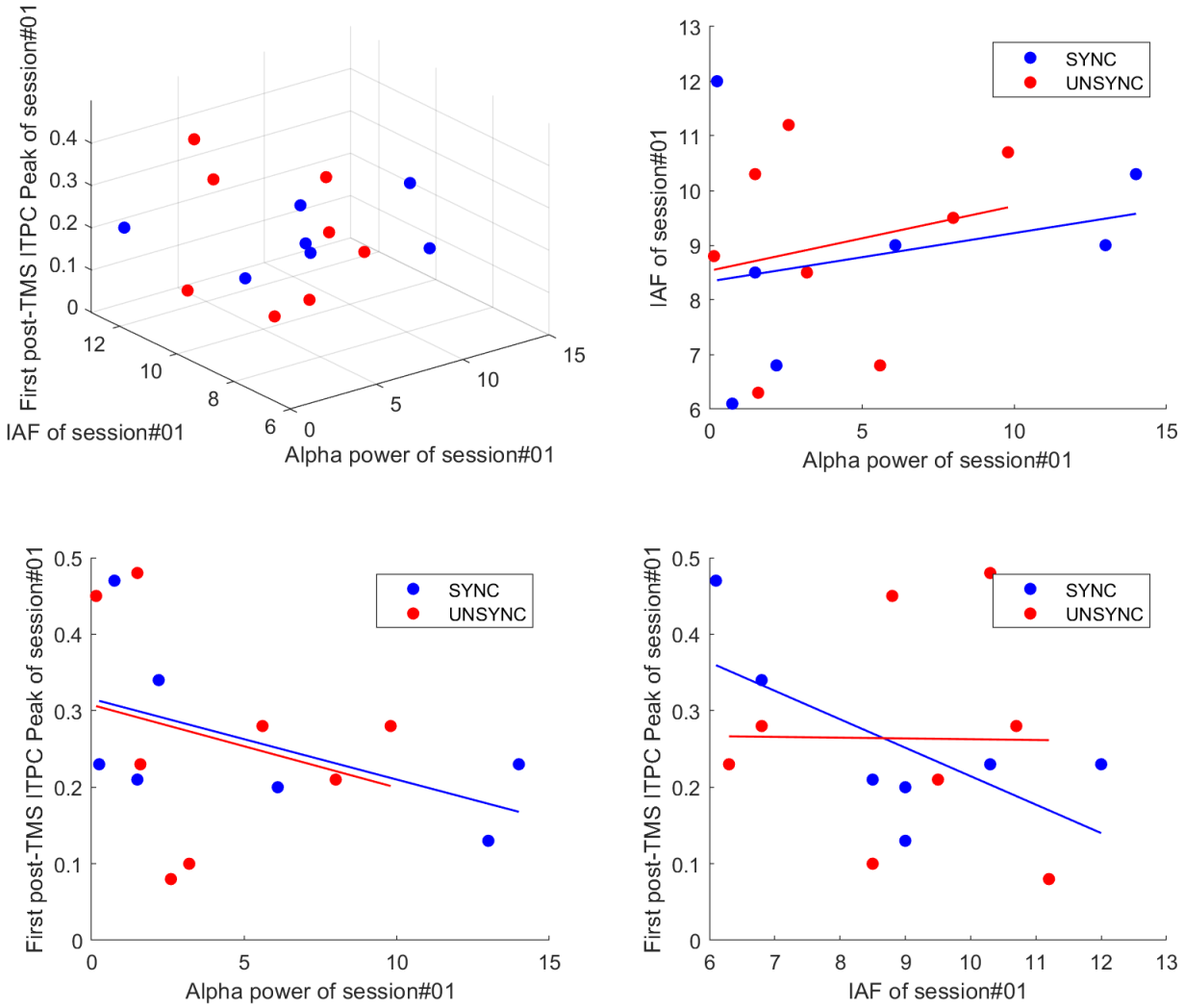

Figure S.4: Distributions of IAF, quasi-alpha power(resting) and post-TMS phase entrainment in different dimension. From top to down, left to right, the distributions of IAF, quasi-alpha power and first post-TMS ITPC peak of session #01 are shown and tested for their possible correlations between each other. The fitting lines (SYNC: blue and UNSYNC: red) are plotted as well, whereas none of their correlations is significant ($p > 0.05$, see Table S.2 for correlation result).

power on the post-TMS phase entrainment, we chose the first session from all subjects (which can be viewed as a baseline regardless of the possible effects from different long-term rTMS treatments) and test for the correlations between IAF, ITPC$^{max[1]}$ and the power spectrum at the calculated IAF.

First, the result of an unpaired t-test between the associated quasi-alpha power of the SYNC and the UNSYNC group shows there is no significant difference between them ($p = 0.5902$). The correlation between the IAF and its associated power (that is computed during the first 5-minute resting state) of each group has been calculated ($p_{sync} = 0.57$ and $p_{unsync} = 0.59$, see Table S.2), and neither of the groups show that the value of the IAF and its associated power is significantly linearly correlated (e.g., lower IAF value would associate with a high power). Furthermore, for other correlation tests between quasi-alpha power and ITPC$^{max[1]}$, and between IAF and ITPC$^{max[1]}$ for

each condition, none show significant linear correlation (see Table S.2 and Figure S.4). All these results show that the increased phase entrainment after phase-locked rTMS treatment is less likely to be caused by the resting power at the calculated IAF or the low IAF itself. However, because of the small sample size in each group, the interpretation of these results has low power and is difficult to make strong conclusions from. A more thorough analysis would require more subjects.

S.5 Accuracy of phase-locked rTMS triggering

Because our experiment uses a rTMS pulse train that contains multiple continuous TMS pulses, after alpha band filtering, the filtered data would introduce a long period of TMS artifacts (around 128 ms). For a single TMS pulse, we can try to recover the instantaneous phase by reconstructing the EEG data up to the point where the TMS pulse is triggered by using TMS artifact removal techniques or by more confidently predicting the phase oscillation within a short time. However, for a rTMS pulse train, this result is not accurate and trustworthy. Therefore, based on current experiment data, the true phase at $t = 0$ s, where the first TMS pulse within a rTMS pulse train is triggered, cannot be accurately recovered offline to report the phase targeting accuracy directly. Fortunately, in our previous work we designed a real-time EEG phase-locked system that fired single TMS pulses[7], where we could recover the phase for accuracy reporting. Similar to how other works that contain phase calculations report their accuracy (e.g., the phase estimation work of Blackwood et al. [5], and the closed-loop phase targeting work of Zrenner et al.[6]), in our previous study, we reported 74.4 to 95.5% of pulses were triggered within $\pm$ 90° of the targeted phase[7]. The phase targeting system presented in this paper is an improvement on the methods used in our prior work, and was specified to achieve accuracy at least within $\pm$ 90° of the targeted phase as well.

Sub	Condition	Target phase	# of triggers	$\mu \pm \sigma(\phi)$	error(ϕ)
P09	sync	174°	27	142° $\pm$ 71°	77°
P10	sync	100°	29	99° $\pm$ 72°	65°
P11	sync	177°	28	250° $\pm$ 66°	77°
P12	sync	355°	34	97° $\pm$ 60°	95°
P13	sync	29°	24	211° $\pm$ 69°	74°
P14	sync	64°	31	226° $\pm$ 73°	74°
P15	sync	23°	34	140° $\pm$ 71°	84°

Table S.3: Summary of phase triggering accuracy for all SYNC subjects. Column *Target phase* is the phase we targeted when the rTMS-EEG system triggered. Column *# of triggers* shows how many trigger attempts were made during the EEG-rTMS system simulation on the 5-min pre-treatment resting data from two selected sessions. Column $\mu \pm \sigma(\phi)$ shows the mean and standard deviation of the recovered phases at the time of triggering. Column *error(ϕ)* is the average phase difference between the recovered phases and the individual target phase. The average of the error (ϕ) across all reported SYNC subjects is 78°.

To further investigate the phase targeting accuracy of the current system without the effects of TMS artifacts, we reran the EEG-rTMS treatment system using the 5-min pre-treatment resting state data sets as inputs. These simulations were run for each SYNC subject for Session #4 and Session #25. These sessions were chosen to represent the accuracy measurement around the beginning and the end of the entire treatment and account for session variation and possible improvement of triggering accuracy (e.g., alpha oscillation becomes more stable towards the end which results in better target phase estimation). The EEG-rTMS system simulations were run

using the same parameters (IAF and RMSE) as rTMS treatment Sessions #4 and #25. The full system was run with the Magstim TMS device shut down, so real rTMS pulse train triggers were produced and recorded with event markers in the data file, but without the EEG artifacts from rTMS device pulses. We computed the EEG phase at the trigger event marker, compared it with the individual target phase, and obtained an estimate of triggering accuracy. The results showed no significant difference in triggering accuracy between Session #4 and Session #25 for the SYNC subjects, so the triggering events from the two sessions were merged to generate the triggering accuracy report (see Table S.3). The error(ϕ) column in Table S.3 is the average difference between all recovered phases and the target phase. For example, Sub #P09 has an error(ϕ) = 77°, which means the pulses were triggered within ±77° of the target phase 174°. According to the results, the average error(ϕ) across all SYNC subjects is 78°, which means that pulses were triggered within ±78° of the target phase, which is a slight improvement (i.e., 12°) compared to our previous system results, but not as good as the phase-locking system introduced in Zrenner's work [6] where they only targeted two phases and their phase estimation accuracy is ±53° if targeted at positive peak (i.e., 0°) and ±55° if targeted at negative peak (i.e., 180°).

S.6 Inter-pulse train interval

In our closed-loop EEG-rTMS system, the time length of the inter-pulse train (i.e., the time length of the **Pre** dataset) is completely dependent on the time when the next target phase (ϕ_{targ}) can be accurately determined. This is determined by the phase prediction fitting model, which is relevant to the corresponding power (e.g., high quasi-alpha power will have more accurate quasi-alpha phase prediction). Therefore, based on the nature of the inter-pulse train interval (i.e., when will the next TMS pulse train triggering event happen), the distribution of interval length per trial should be a Poisson distribution (positively skewed) instead of a normal distribution, because a Poisson distribution expresses the probability of a given number of events occurring in a fixed interval of time or space if these events occur with a known constant mean rate and independently of the time since the last event[13].

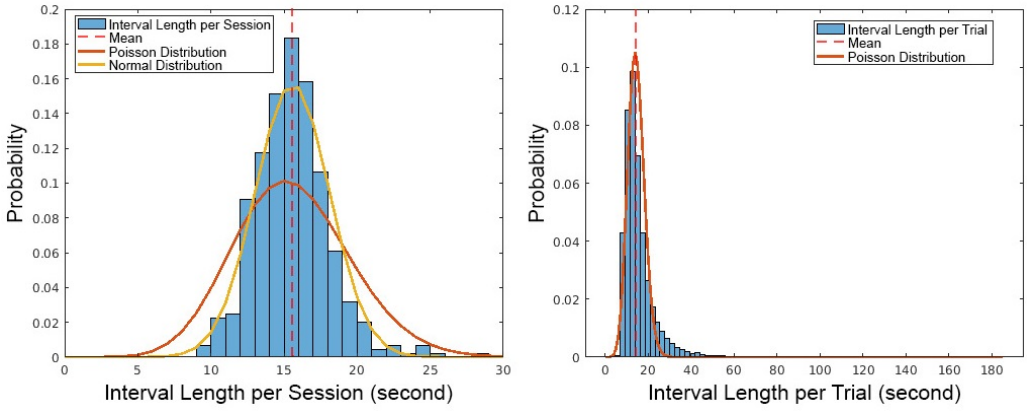

Figure S.5: Distribution of inter-pulse train interval length. On the left, it shows the histogram of interval length per session, and on the right, it shows the histogram of interval length per trial. By its definition, the interval length per trial should be a Poisson distribution, so it is positively skewed compared to the interval length per session, which is a normal distribution. Because interval length per session is obtained by calculating the mean of inter-pulse train interval length within one session, the interval length per session is clustered around the mean (15.6 seconds) with a smaller range between 9.7 to 28.2 seconds.

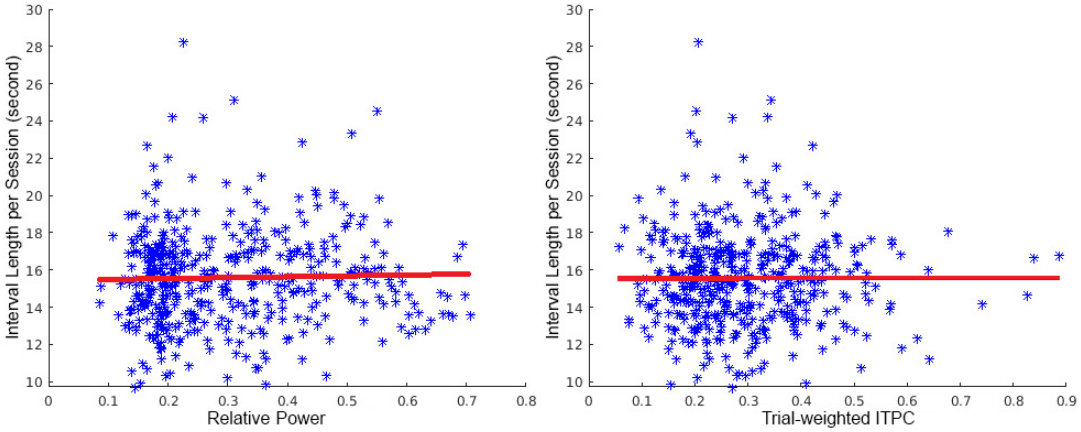

Figure S.6: Correlation between inter-pulse train interval length per session and relative quasi-alpha power/trial-weighted ITPC$^{[1]}_{max}$. On the left, the Pearson's test (fitted with red line, $\rho = 0.04, p = 0.42$) shows that there is no linear correlation between interval length per session and relative power. One the right, the Pearson's test (fitted with red line, $\rho = 0.01, p = 0.88$) shows that there is no linear correlation between interval length per session and trial-weighted ITPC$^{[1]}_{max}$.

From the observation of the histogram (see Figure S.5), we can see that the distribution of inter-pulse train length by trial does belong to a Poisson distribution with mean equal to 15.6 seconds with a range between 2.5 to 186 seconds as we mentioned in our main manuscript (trials with interval length less than 2.5 seconds are excluded from the analysis). However, since the concept of ITPC and the computation of relative quasi-alpha power are based on session, interval length per session is also calculated by averaging interval length of all trials within each session for correlation analysis. We can see that the interval length per session (i.e., session average) is a normal distribution with the same mean value 15.6 seconds and standard deviation of 2.5 seconds (see Figure S.5).

Because the determination of interval length is possibly related to the quasi-alpha power which is associated with the target frequency oscillation, we investigated the correlation between interval length and relative power ($\bar{\alpha_P}$) that we used for the trial weighting. In addition, we tested the correlation between interval length and trial-weighted ITPC$^{max[1]}$ to see whether the length of inter-pulse train interval would be a possible confound for our generalized linear mixed model (GLMM) with Pearson's correlation test. In Figure S.6, on the left side, it shows that there is no correlation between interval length per session and relative power($\rho = 0.04, p = 0.42$). Moreover, on the right side, according to Pearson's correlation test result, there is no linear correlation between interval length per session and trial-weighted ITPC$^{max[1]}$ either ($\rho = -0.01, p = 0.88$).

S.7 Identifying first post stimulation peak in ITPC

The brain synchronization represented by phase entrainment in the quasi-alpha band in our study is seen as the level of phase alignment in the EEG post-TMS stimulation across all (i.e., 75) trials per session, here measured by ITPC (see Figure 4 in main manuscript). The larger the ITPC value, the more consistent is the EEG phase across trials after the TMS pulse train has ended. We define the first post-stimulation ITPC peak (ITPC$^{max[1]}$) as the first local maximum of the ITPC following the last TMS pulse in a train (see Figure 3 in main manuscript). For this peak, we required that it was also the local maximum in a window from -25 to +25 ms centered

at the peak. The first 128 ms and last 128 ms were not analyzed as we expected quasi-alpha-band filtering artifacts caused by zero padding at the beginning and end of the **Post** epoch. This time window was determined by the order of the filter and the sampling rate (marked as filter edge in Figure 3 of the main manuscript, only the first filter edge was listed here because only $t \in [0, 2]$s was shown in the plot for the post stimulation ITPC). Specifically, $\text{ITPC}^{max[1]}$ for each individual was always detected between 128 ms and 600 ms after the last TMS pulse in a pulse train. We focused on $\text{ITPC}^{max[1]}$ because it shows the immediate changes of the level of brain synchronization after the TMS pulse train. By analyzing $\text{ITPC}^{max[1]}$ from each session, we can investigate how brain synchronization immediately after the TMS pulse train changes across sessions, and most importantly, whether there is a difference between SYNC and UNSYNC groups. Performing this analysis for each session enabled us to track long-term changes of brain synchronization post rTMS across sessions (see Figure 3 in main manuscript).

S.8 Further discussion of GLMM result

In Table 4 in the main manuscript, the interaction term between the relative quasi-alpha power and the treatment condition ($\bar{\alpha_P} : condition$) in the GLMM is not significant at a significance level of 0.05 ($p_{(\bar{\alpha_P}:condition)} = 0.0668$), but it is very close to the threshold, so it is helpful to investigate this effect from the interaction term $\bar{\alpha_P} : condition$. In Figure S.7, the model predictions of changes in $\text{ITPC}^{max[1]}$ with respect to $\bar{\alpha_P}$ in the two groups are shown. In both the SYNC and UNSYNC group, as the GLMM result suggests, there is a non-significant negative relationship between relative power and $\text{ITPC}^{max[1]}$ (see Table 4 in the main manuscript). With the interaction term of treatment groups combined, then we can observe this small and insignificant difference in $\text{ITPC}^{max[1]}$ with different values of $\bar{\alpha_P}$, where the UNSYNC group has a slightly higher value of $\text{ITPC}^{max[1]}$ under the same relative quasi-alpha power (see Figure S.7, $\text{ITPC}^{max[1]}_{unsync,\min(\bar{\alpha_P})} - \text{ITPC}^{max[1]}_{sync,\min(\bar{\alpha_P})} = 0.05$; $\text{ITPC}^{max[1]}_{unsync,\max(\bar{\alpha_P})} - \text{ITPC}^{max[1]}_{sync,\max(\bar{\alpha_P})} = 0.05$, where $\min(\bar{\alpha_P}) = 0.09$ and $\max(\bar{\alpha_P}) = 0.71$)

Additionally, to investigate the possible correlation between $\bar{\alpha_P}$ and session for different conditions (e.g., SYNC group will have an increase or decrease in $\bar{\alpha_P}$ with the session increase), we use Spearman's ρ to test the correlation between those two variables. According to the correlation result, neither the SYNC nor UNSYNC group has a significant correlation between $\bar{\alpha_P}$ and session ($\rho_{sync} = 0.0947$, $p_{sync} = 0.1781$; $\rho_{unsync} = -0.0087$, $p_{unsync} = 0.8940$, see Figure S.8). Additionally, although from Figure S.8 we can observe that the fitting line for the $\bar{\alpha_P}$ of the UNSYNC group has a greater value compared to the SYNC group, when we test this difference of distribution by session, there is no significant difference between $\bar{\alpha_P}$ in the SYNC and UNSYNC group across session.

Name	Estimate	SE	t-Stat.	DF	p-Value	Lower CI	Upper CI
(Intercept)	-0.9829	0.3202	-3.0694	435	0.0023	-1.6123	-0.3535
stimf	0.0129	0.0236	0.5498	435	0.5827	-0.0333	0.0592
$\bar{\alpha_P}$	-0.2405	0.5605	-0.4291	435	0.6681	-1.3420	0.8611
session	0.0055	0.0034	1.5981	435	0.1108	-0.0013	0.0122
condition	-0.0456	0.3053	-0.1494	435	0.8813	-0.6457	0.5544
$\bar{\alpha_P}$:condition	-0.7630	0.7736	-0.9863	435	0.3245	-2.2833	0.7574
session:condition	0.0090	0.0052	1.7231	435	0.0856	-0.0013	0.0193

Table S.4: Fixed effects coefficients (95% CIs) of GLMM with non-power weighted inter-trial phase coherence for near target region (i.e., electrode F3, FP1, and F7).

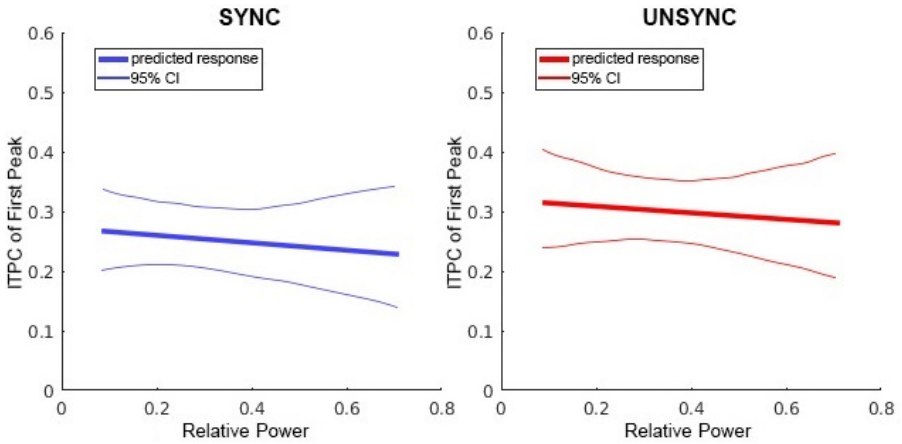

Figure S.7: The model prediction of changes in ITPC$^{max[1]}$ among different relative quasi-alpha powers ($\bar{\alpha_P}$) for SYNC and UNSYNC groups at the ROI near the rTMS target region. We can observe that there is a small trend in the prediction that with the increase of $\bar{\alpha_P}$, the value of predicted ITPC$^{max[1]}$ would decrease in both SYNC (ΔITPC $= -0.04$) and UNSYNC group (ΔITPC $= -0.03$). However, with the 95% confidence interval combined, we can see that there is no significant changes in ITPC$^{max[1]}$ with the increase/decrease of $\bar{\alpha_P}$ in both groups. This might happen because we have less samples with a high value of $\bar{\alpha_P}$. Additionally, although the model prediction shows that with the same $\bar{\alpha_P}$, UNSYNC group will have a higher value of ITPC$^{max[1]}$ compared to the SYNC group, but it is not significant under 95% confidence level.

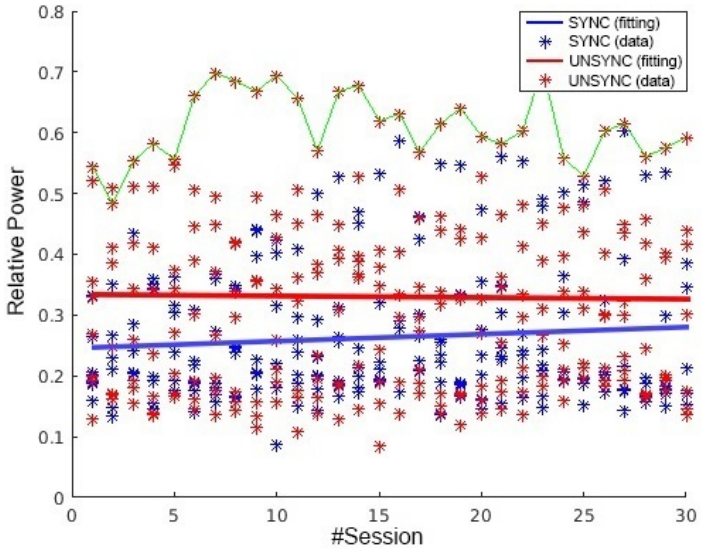

Figure S.8: Pearson's correlation between #session and relative quasi-alpha power for each treatment group. SYNC group is shown with blue color and UNSYNC group is shown with red color. Fitting lines of both SYNC and UNSYNC are shown ($\rho_{sync} = 0.0947$, $p_{sync} = 0.1781$; $\rho_{unsync} = -0.0087$, $p_{unsync} = 0.8940$). Additionally, one UNSYNC subject (#P01) who has a overall high value of relative power is highlighted with green line. Even though we can see that the fitting line for UNSYNC group has a higher value of relative quasi-alpha power than SYNC group, t-test by session did not show any difference between SYNC and UNSYNC group by session.

Lastly, we reran our GLMM with no weighting applied with ITPC$^{max[1]}$ as the dependent variable for the near target region. We can see that there is still an effect of the interaction

between session (i.e., session#1 to #30) and condition (i.e., SYNC and UNSYNC group), though the associated p-values are not as low as the GLMM result with weighted ITPC ($p = 0.0856$). Moreover, we still observe the trend ($p = 0.1108$) that there is an increase in quasi-alpha phase synchronization with an increase in session number. Additionally, the UNSYNC subject who has a significant increase of $\text{ITPC}^{max[1]}$ is the subject who has the highest $\bar{\alpha_P}$ measured for inter-pulse interval (Subject #P01, see Figure S.8). This suggests that the change in neuroplasticity is indirectly mediated by the different modulation of the power across sessions between SYNC and UNSYNC patients with the phase-locked rTMS treatment. However, because of the limited sample size, we cannot further test or conclude anything about the effect of relative quasi-alpha power.

S.9 Power spectrum within IAF frequency range (6 to 13 Hz)

Changes in the spectral power with respect to the defined IAF (6 to 13Hz) were computed for four ROIs (near rTMS target, contralateral to rTMS target, medial-frontal, and occipital region) for SYNC and UNSYNC subjects. Consistent with the time window used for post-stimulation ITPC peak detection, we compared the difference in spectral power between pre-stimulation and post-stimulation measurements between the two groups, covering a latency of 128 ms to 2000 ms before and after the rTMS pulse train.

The spectrum is calculated using the Welch method (window size of 128 samples with no overlap between windows). For comparison, the difference between the mean of the pre- and post-stimulation log-transformed power spectral density within the frequency range of 6 to 13 Hz was computed for each week of treatment. The average of three electrodes' power spectrum within each ROI is used to represent the power spectrum within that region (e.g., near to rTMS target region includes electrode FP1, F3, and F7). No significant weekly increase or decrease of power spectrum changes between pre- and post-stimulation were found. In Figure S.9, the power spectrum changes between pre- and post-stimulation of week 1 and week 6 for each group are presented. Compared to the pre-stimulation, there is a significant (within 95% confidence interval) increase between pre- and post-stimulation measurements in the signal's power spectrum within the IAF frequency range in the SYNC condition for all three ROIs ($p_{tar} = 0.05$, $p_{med} = 0.05$, $p_{contra} = 0.03$). This is consistent with the finding by Zrenner et al. [20] that there is a significant difference between baseline and post-stimulation measurements in the signal's power spectrum within the frequency range of 11 to 14 Hz in the alpha-synchronized rTMS condition in the electrodes around target and medial-frontal region. However, this significant increase of power after the rTMS pulse trains was not observed in the UNSYNC group. Even though differences in the power spectrum changes after rTMS pulse train between the SYNC and UNSYNC groups were found, ultimately there is no significant difference in power spectrum changes between these groups in both week 1 and week 6 (see Figure S.9).

S.10 Source of quasi-alpha oscillation

One possible limitation in our study is that there are multiple factors that can call into question whether the frontal quasi-alpha signal in our findings is really generated from frontal regions or instead posterior regions transmitted by volume conduction to the frontal EEG electrodes. Recording EEG with a low-density cap (i.e., 32 electrodes), analyzing at the sensor level, and obtaining EEG data at rest can all increase the signal to noise ratio (SNR) of the quasi-alpha band for posterior regions[14]. A study showed that the oscillatory response to TMS depended on the stimulated

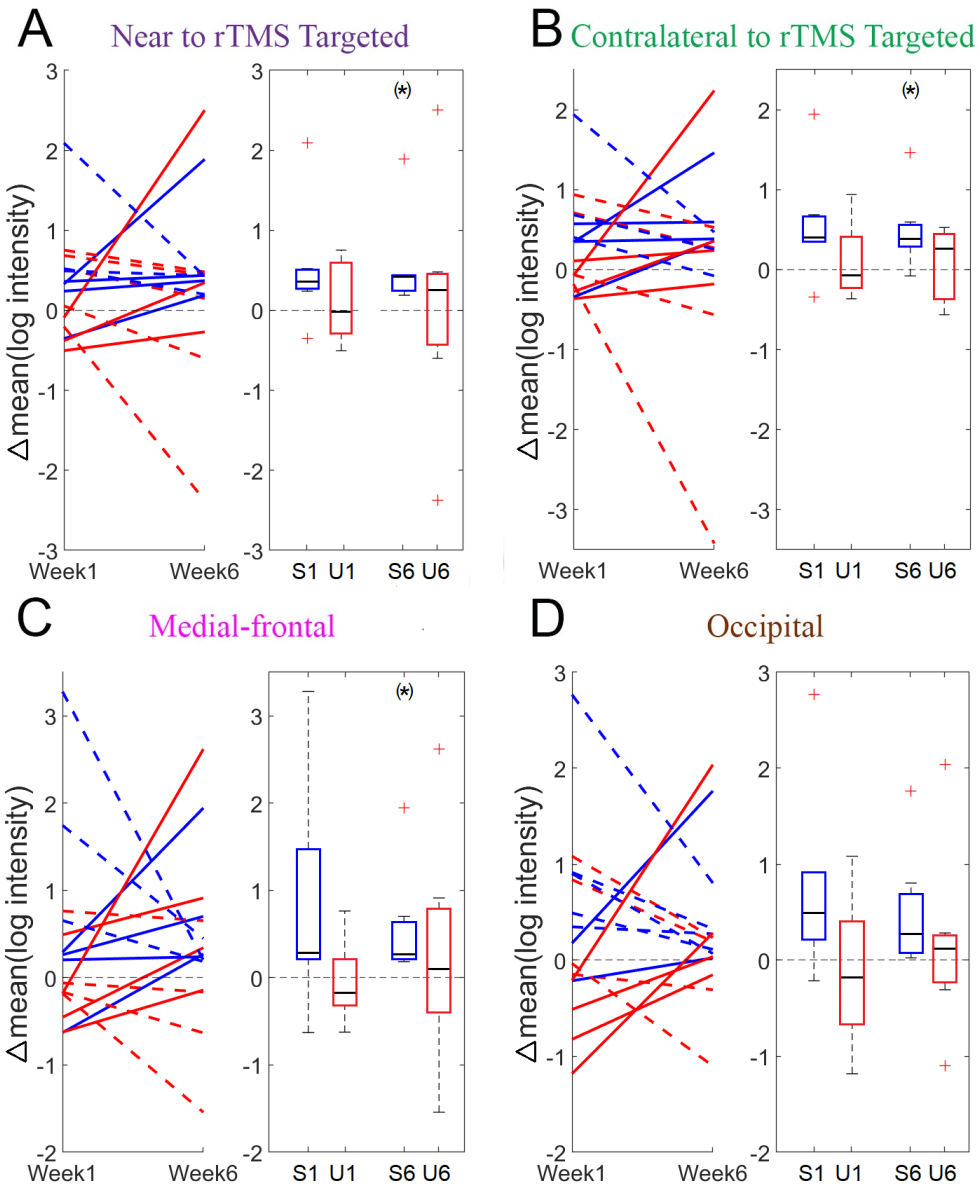

Figure S.9: Plots of the difference in the mean of log power spectrum density between pre- and post-stimulation measurements in the SYNC and UNSYNC condition. Frequency range of 6 to 13 Hz (i.e., IAF) is included. Asterisks correspond to the #week in each group pertaining to the statistically significant power increases between pre- and post-stimulation at 95% confidence level. For instance, subplot **(A)** shows the power spectrum difference between pre- and post-stimulation for week 1 and week 6 in subject-level (line plot on the left) and group-level (box plot on the right). On the left, each line is an individual subject (SYNC: blue, UNSYNC: red). A solid line indicates there is an increase of $\Delta \log(PSD)$ between week 1 and week 6, while a dash line indicates a decrease. Boxplots of data from week 1 and week 6 of each group are shown on the right, asterisks on top means the corresponding p-values of t-test is less than 0.05, where the null hypothesis is that the data comes from a normal distribution with mean equal to zero and unknown variance. For example, (*) on S6 means there is a significant increase in the power spectrum within the 6 to 13 Hz frequency range between pre- and post-stimulation 2s time window for the SYNC group, week 6). Subplot **(B)**, **(C)** and **(D)** are similar to **(A)**, except that the comparison is performed for different ROIs.

cortex[15], as prefrontal TMS induced a brief high beta oscillation. Alpha-band power increases were actually characteristic of posterior cortex stimulation[6, 16].

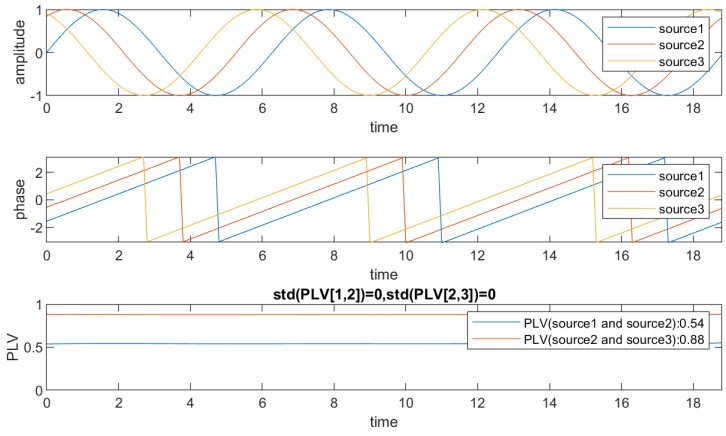

Figure S.10: Phase locking value (PLV) and standard deviation of PLV calculated based on synthetic data. As shown in the subplot on the top, there are three identical oscillations (sine wave) with different time delays (i.e., source1, source2, and source3). Their corresponding phases are plotted in the middle and the PLVs between source1 and source2 (PLV[1,2] = 0.54), and source2 and source3 (PLV[2,3] = 0.88) on the bottom. As we can see, since source1, source2 and source3 are identical oscillations with different time delays, the standard deviation of the PLV value between two sources is around 0 ($\sigma(C) = 0$, where C is a constant number), while the PLV itself is less informative (different PLVs are obtained between two sources, but all three oscillations are same oscillations with different time delays).

In order to further understand this quasi-alpha oscillation that we detected in different ROIs and rule out the possibility of volume conduction, we applied the phase locking value (PLV) to compare the quasi-alpha oscillation between sensors. PLV is a measure of the phase synchronization between two time-series from two different sensors, which has been previously applied to connectivity analysis between regions [17, 18]. The PLV measurement of phase synchronization takes values between 0 and 1, where 0 indicates there is no phase synchrony and 1 indicates the relative phase between the two signals is identical in that trial [18]. PLV measures whether the signals from two electrodes can be related by a linear time invariant transformation, in other words a constant amplitude ratio and phase shift (delay) [19]. This means if the quasi-alpha oscillations from two electrodes are generated from the same source, the PLV should be approximately constant, since the phase lag between two oscillations from the same source should be constant which means the standard deviation of the phase lag equals 0 (i.e., $\sigma(C) = 0$, where C is a constant number, see Figure S.10). Particularly, we examined the phase synchronization of the quasi-alpha oscillations between the target electrode (F3) and an electrode from the occipital region (Oz), as well as between the target electrode (F3) and an electrode near the right mastoid reference (P8) to show whether those oscillations came from the same source. Additionally, electrodes near the primary motor cortex (M1) (C3 and C4) have been investigated, because sensory-motor cortex might be a considerable source of the quasi-alpha band signal close to the cortical area of interest (i.e., DLPFC). Here, we discuss the results of the two subjects with the most significant increase in $\text{ITPC}^{max[1]}$ across sessions as an example (one subject from each treatment group, UNSYNC #P01 and SYNC #P09, summary of all subjects are available in Table S.5).

We first compare the phase synchronization between the TMS target electrode (F3) and the near right mastoid reference electrode (P8). PLV is calculated between electrodes F3 and P8 for

Sub	Condition	$(F3, Oz)$	$(F3, P8)$	$(F3, C3)$	$(F3, C4)$
P01	unsync	98.76%	99.56%	53.58%	65.01%
P02	unsync	99.10%	99.50%	64.09%	88.70%
P03	unsync	98.67%	98.67%	79.01%	96.13%
P04	unsync	97.10%	97.77%	80.29%	89.52%
P05	unsync	98.75%	96.92%	80.71%	92.01%
P06	unsync	97.32%	99.23%	57.05%	62.06%
P07	unsync	99.23%	99.33%	59.79%	77.74%
P08	unsync	89.94%	97.85%	45.91%	74.88%
P09	sync	96.33%	96.02%	75.93%	90.47%
P10	sync	97.29%	99.24%	83.96%	91.06%
P11	sync	85.82%	98.91%	66.21%	77.92%
P12	sync	90.55%	96.75%	64.08%	80.84%
P13	sync	96.00%	99.51%	62.80%	58.34%
P14	sync	100.00%	100.00%	61.42%	86.65%
P15	sync	98.53%	98.89%	79.16%	89.42%

Table S.5: Summary of trial percentage that has standard deviation of PLV greater than 0.1 for all subjects. Results calculated between F3 and four representative electrodes (i.e., Oz, $P8$, $C3$, and $C4$) are presented. Higher percentage means less trials have identical oscillations between two sources (less alignment) and lower percentage indicates more trials have phase alignment between sources (greater alignment).

UNSYNC subject #P01, using a time window from 0.128 to 1 second past the last (40^{th}) TMS pulse within a rTMS pulse train. This is the same time window in which the first post-rTMS ITPC peak ($\text{ITPC}^{max[1]}$) had been detected. Overall, for all sessions from subject #P01, there are 99.56% trials that have a standard deviation greater than 0.1 for the PLV in the selected time window, which means only very few trials among all sessions have a relatively constant PLV for the same post-rTMS time window that we used for ITPC peak detection. The fact that the PLV varies substantially between 0 and 1 means that there is no constant phase shift between electrodes F3 and P8. This in turn suggests that these electrodes are measuring two different alpha oscillations and F3's signal is not entirely the result of volume conduction from a source near P8.

For the SYNC subject #P09, we have similar findings. For all sessions from subject #P09, there are 96.02% trials that have a standard deviation greater than 0.1 for the PLV on this selected time window. Similarly, using the same methodology, we investigated the phase synchronization between the target electrode (F3) and an electrode over the occipital region (Oz). These results also suggest that it is less likely that this target oscillations in those two regions come from the same source. In this case for UNSYNC subject #P01, 98.76% trials of all sessions have a standard deviation greater than 0.1, and for SYNC subject #P09, 96.33% trials of all sessions have a standard deviation greater than 0.1. For electrodes near the motor cortex (C3 and C4), the result is mixed. For UNSYNC subject #P01, only 53.58% and 65.01% of trials' standard deviation of PLV calculated between F3 and C3 and between F3 and C4 are greater than 0.1 (i.e., F3 and C3/C4 are highly synchronized), which means, for this subject, it is likely that his or her source of target oscillation detected at prefrontal region is generated from motor cortex or the effect of volume conduction from F3 to C3/C4 is strong for this subject (even though both C3 and C4 are synchronized with F3, the percentage increases with the increase of distance to F3). For SYNC subject #P09, 75.93% and 90.47% of trials' standard deviation of PLV calculated between F3 and C3 and between F3 and C4 are greater than 0.1 (i.e., F3 and C3 are relatively synchronized, but not with C4), which means,

for this subject, it is more unlikely that his or her source of quasi-alpha oscillation detected at the prefrontal region is generated from the motor cortex. The relatively low percentage observed between F3 and C3 might be caused by the effect of volume conduction from F3 to C3 (even though C3 are likely synchronized with F3, the percentage between F3 and C4 is high). In summary, these results suggest that the alpha oscillation we phase lock to and measured in the prefrontal cortex is not due to volume conduction of an alpha source in occipital or parietal cortex, but for subjects (i.e., #P01, #P06, #P07, #P08, #P13) who have low percentage values measured between F3 and C3/C4, it is possible that the source of oscillation is from the motor cortex. For subject #P13, it is very likely that the source of detected oscillation comes from the motor cortex, because the trial percentage between F3 and C4 is smaller than trial percentage between F3 and C3 (not follow the volume conduction propriety that the effects of recording electrical potentials at a near distance from their source generator more likely be stronger). However, for subject #P01, #P06, #P07, #P08, more investigation would be needed to verify this.

References

[1] Goldman, R. I., Wei, C.-Y., Philiastides, M. G., Gerson, A. D., Friedman, D., Brown, T. R., and Sajda, P. *Single-trial discrimination for integrating simultaneous eeg and fmri: identifying cortical areascontributing to trial-to-trial variability in the auditory oddball task*. Neuroimage, 47(1):136–147, 2009.

[2] Sajda, P., Goldman, R. I., Dyrholm, M., and Brown, T. R. *Signal processing and machine learningfor single-trial analysis of simultaneously acquired eeg and fmri*. Statistical signal processing for neuroscience and neurotechnology, pages 311–334, 2010.

[3] Walz, J. M., Goldman, R. I., Carapezza, M., Muraskin, J., Brown, T. R., and Sajda, P. *Prestimulus eeg alpha oscillations modulate task-related fmri bold responses to auditory stimuli* . NeuroImage, 113:153–163, 2015.

[4] George, M and Saber, G and McIntosh, J and Doose, J and Faller, J and Lin, Y and Moss, H and Goldman, R and Sajda, P and Brown, T *Combined TMS-EEG-fMRI. The level of TMS-evoked activation in anterior cingulate cortex depends on timing of TMS delivery relative to frontal alpha phase*. Brain Stimulation: Basic, Translational, and Clinical Research in Neuromodulation, 12(2):580, 2019.

[5] Blackwood, Ethan, Meng-chen Lo, and Alik S. Widge. *Continuous phase estimation for phase-locked neural stimulation using an autoregressive model for signal prediction.* In 2018 40th Annual International Conference of the IEEE Engineering in Medicine and Biology Society (EMBC), pp. 4736-4739. IEEE, 2018.

[6] Zrenner, Christoph, Debora Desideri, Paolo Belardinelli, and Ulf Ziemann. *Real-time EEG-defined excitability states determine efficacy of TMS-induced plasticity in human motor cortex.* Brain stimulation 11, no. 2 (2018): 374-389.

[7] Josef Faller, Yida Lin, Jayce Doose, Golbarg T. Saber, James R. McIntosh, Joshua B. Teves, Robin I. Goldman, Mark S. George, Paul Sajda, and Truman R. Brown. *An EEG-fMRI-TMS instrument to investigate BOLD response to EEG guided stimulation.* In 2019 9th International IEEE/EMBS Conference on Neural Engineering (NER), pp. 1054-1057. IEEE, 2019.

[8] McIntosh, J. R., and P. Sajda. *Estimation of phase in EEG rhythms for real-time applications.* Journal of neural engineering 17, no. 3: 034002, 2020.

[9] Mishory, Alexander, Christine Molnar, Jejo Koola, Xingbao Li, F. Andrew Kozel, Hugh Myrick, Zachary Stroud, Ziad Nahas, and Mark S. George. *The maximum-likelihood strategy for determining transcranial magnetic stimulation motor threshold, using parameter estimation by sequential testing is faster than conventional methods with similar precision.* The journal of ECT 20, no. 3: 160-165, 2004.

[10] Jasper, Herbert H. *The ten-twenty electrode system of the International Federation.* Electroencephalogr. Clin. Neurophysiol. 10: 370-375, 1958.

[11] Haller, M, Donoghue, T, Peterson, E, Varma, P, Sebastian, P, Gao, R, Noto, T, Knight, RT, Shestyuk, A and Voytek, B *Parameterizing neural power spectra.* BioRxiv, p.299859, 2018.

[12] Donoghue T, Haller M, Peterson EJ, Varma P, Sebastian P, Gao R, Noto T, Lara AH, Wallis JD, Knight RT, Shestyuk A, & Voytek B *Parameterizing neural power spectra into periodic and aperiodic components.* Nature Neuroscience, 23, 1655-1665, 2020.

[13] Haight, Frank A. *Handbook of the Poisson distribution.* No. 519.23 H3. 1967.

[14] Klimesch, Wolfgang. *Alpha-band oscillations, attention, and controlled access to stored information.* Trends in cognitive sciences 16, no. 12 (2012): 606-617.

[15] Rosanova, Mario, Adenauer Casali, Valentina Bellina, Federico Resta, Maurizio Mariotti, and Marcello Massimini. *Natural frequencies of human corticothalamic circuits.* Journal of Neuroscience 29, no. 24 (2009): 7679-7685.

[16] Ronconi, Luca, Niko A. Busch, and David Melcher. *Alpha-band sensory entrainment alters the duration of temporal windows in visual perception.* Scientific reports 8, no. 1 (2018): 1-10.

[17] Ghuman, Avniel Singh, Jonathan R. McDaniel, and Alex Martin. *A wavelet-based method for measuring the oscillatory dynamics of resting-state functional connectivity in MEG.* Neuroimage 56, no. 1 (2011): 69-77.

[18] Aydore, Sergul, Dimitrios Pantazis, and Richard M. Leahy. *A note on the phase locking value and its properties.* Neuroimage 74 (2013): 231-244.

[19] Srinivasan, Ramesh, William R. Winter, Jian Ding, and Paul L. Nunez. *EEG and MEG coherence: measures of functional connectivity at distinct spatial scales of neocortical dynamics.* Journal of neuroscience methods 166, no. 1 (2007): 41-52.

[20] Zrenner, Brigitte, Christoph Zrenner, Pedro Caldana Gordon, Paolo Belardinelli, Eric J. McDermott, Surjo R. Soekadar, Andreas J. Fallgatter, Ulf Ziemann, and Florian Müller-Dahlhaus. *Brain oscillation-synchronized stimulation of the left dorsolateral prefrontal cortex in depression using real-time EEG-triggered TMS.* Brain stimulation 13, no. 1 (2020): 197-205.